International Journal of Nanomedicine

Dovepress
open access to scientific and medical research

Open Access Full Text Article

ORIGINAL RESEARCH

Silver nanoparticle/chitosan oligosaccharide/poly(vinyl alcohol) nanofibers as wound dressings: a preclinical study

This article was published in the following Dove Press journal:
International Journal of Nanomedicine
31 October 2013
Number of times this article has been viewed

Chenwen Li[1,*]
Ruoqiu Fu[1,*]
Caiping Yu[1]
Zhuoheng Li[1]
Haiyan Guan[1]
Daqiang Hu[1]
Dehua Zhao[2]
Laichun Lu[1]

[1]Department of Pharmacy, Institute of Surgery Research, Daping Hospital, Third Military Medical University, [2]College of Pharmacy, Chongqing Medical University, Chongqing, People's Republic of China

*These authors contributed equally to this work

Abstract: In this study, a mixture of poly(vinyl alcohol) (PVA) and chitosan oligosaccharides (COS) was electrospun with silver nanoparticles (AgNPs) to produce fibrous mats for use in wound healing. The AgNPs were reduced by COS prior to electrospinning or Ag^+ was reduced via ultraviolet irradiation in nanofibers. The morphologies of the PVA/COS/$AgNO_3$ and PVA/COS-AgNP nanofibers were analyzed by scanning electron microscopy. Formation of the AgNPs was investigated by field emission transmission electron microscopy, ultraviolet-visible spectroscopy, Fourier transform infrared spectroscopy, and X-ray diffraction. We also evaluated the biocompatibility of the nanofibers, particularly their cytotoxicity to human skin fibroblasts and potential to cause primary skin irritation. The in vitro antibacterial activity and in vivo wound healing capacity of the nanofibers were also investigated. The nanofibers had a smooth surface with an average diameter of 130–192 nm. The diameters of the AgNPs were in the range of 15–22 nm. The nanofibers significantly inhibited growth of *Escherichia coli* and *Staphylococcus aureus* bacteria. PVA/COS-AgNP nanofibers accelerated the rate of wound healing over that of the control (gauze). The results of our in vitro and in vivo animal experiments suggest that PVA/COS-AgNP nanofibers should be of greater interest than PVA/COS/$AgNO_3$ nanofibers for clinical use as a bioactive wound dressing.

Keywords: preclinical study, wound dressing, electrospinning, silver nanoparticles, poly(vinyl alcohol), chitosan oligosaccharides

Introduction

In the field of wound care and management, wound dressings have been widely investigated. The goals of wound dressing include protection, removal of exudates, inhibition of invasion by exogenous microorganisms, and improved skin appearance. An ideal wound dressing should be biocompatible and biodegradable, enhance the healing process,[1] be able to swell for absorption of excess exudates, and have high porosity for respiration. Traditional dressings, such as natural or synthetic bandages, cotton wool, lint, and gauze, all with varying degrees of absorbency, have been used for the management of wounds, but have limited swelling capacity and moisture vapor permeability. To address this issue, nanofibrous membranes produced via electrospinning are beginning to emerge as wound dressing materials, due to their close structural resemblance to the native extracellular matrix, their high surface area-to-volume ratio, and good porosity.[2,3]

Various materials, such as polythene and polycaprolactone,[4] have been designed to produce wound dressings. However, a common drawback of such materials that would discourage their use in the clinical setting involves the use of potentially

Correspondence: Laichun Lu
Department of Pharmacy, Institute of Surgery Research, Daping Hospital, Third Military Medical University, 10 Changjiangzhilu, Chongqing 400042, People's Republic of China
Tel +86 23 6875 7091
Fax +86 23 6875 7091
Email lulaicq@163.com

allergenic materials or organic solvents in the manufacturing process. Because of this problem, the practical use of such conventional wound dressings in the clinical setting is limited. Poly(vinyl alcohol) (PVA) is a biodegradable polyester that has been investigated extensively as a biomedical material. Many researchers have utilized electrospinning to fabricate nanofibrous PVA scaffolds for use in wound healing.[5–7] Additionally, chitosan displays unique polycationic, chelating, and film-forming properties due to the presence of active amino and hydroxyl groups. However, the poor solubility of chitosan in common organic solvents and water at physiological pH values (7.2–7.4) has restricted its use in biomedical applications. However, the hydrolyzed products of chitosan (ie, chitosan oligosaccharides [COS]) overcome these limitations, providing wider applications in diverse fields.[8] Combining COS with PVA for electrospinning can reportedly improve fiber uniformity, especially for electrospinning in dilute solutions.[9]

Silver has antimicrobial properties due to its capacity to interact strongly with the thiol group of compounds found in the respiratory enzymes of bacterial cells. Further, silver nanoparticles (AgNPs) display more efficient antimicrobial properties than other salts due to their extremely large surface area, which provides better contact with microorganisms.[10] AgNPs interact with the sulfur-containing proteins in bacterial membranes and phosphorus-containing compounds, such as DNA, within bacterial cells. As a result, AgNPs are effective antiseptic agents for controlling broad-spectrum microbes and antibiotic-resistant bacteria in vitro,[11–13] reducing the potential for bacterial resistance more efficiently than antibiotics. Taken together, the incorporation of AgNPs into wound dressings containing PVA and COS creates a promising candidate for wound management. However, the available preclinical data on such wound dressings in both humans and animals are scarce at present.

The objective of this study was to develop AgNPs containing nanofibers via electrospinning that could be used as ideal wound dressings. We used two methods to reduce Ag^+ ions into AgNPs via electrospinning. First, silver nitrate ($AgNO_3$) was added to an electrospun solution, and the reduced Ag^+ was incorporated into the electrospun nanofibers via ultraviolet irradiation. Second, we applied chemical reduction by COS prior to electrospinning. Physicochemical characterization, biocompatibility, in vitro antibacterial activity, and in vivo wound healing capacity were then investigated to evaluate PVA/COS/$AgNO_3$ and PVA/COS-AgNP nanofibers as ideal wound dressings.

Materials and methods

Materials

PVA (molecular weight 85,000–124,000, 87%–89% hydrolyzed) was obtained from Sigma-Aldrich (St Louis, MO, USA). COS (average molecular weight above 3,000, 100% water-soluble) was purchased from Golden-Shell Pharmaceutical Co, Ltd (Zhejiang, People's Republic of China). The $AgNO_3$ was obtained from Guanghua Sci-Tech Co, Ltd (Guangzhou, People's Republic of China). All reagents were of analytical grade and used without further purification. Double-distilled water was used to prepare all polymer solutions.

Synthesis of COS-Ag nanoparticles

The COS-AgNPs were prepared by stirring 35 mL of a 0.1 M $AgNO_3$ solution containing 1 g COS for 5 hours at 50°C. When the color of the solution changed from colorless to brown, signifying the formation of AgNPs, the reaction vessel was cooled to room temperature. Two volumes of acetone were added to precipitate the product, which was then dried at 100°C under a vacuum for 24 hours.

The quantity of silver present in the COS-AgNPs was determined by dissolving 5 mg of the sample in 10 mL of 50% nitric acid (HNO_3). The volume was then adjusted to 100 mL using double-distilled water as a releasing medium. The silver concentration was measured via atomic absorption spectroscopy, and the results are reported as average values (n=3).

Preparation and characterization of electrospinning solutions

A 3% (w/v) COS solution was prepared by dissolving COS powder in distilled water at room temperature with magnetic stirring for 1 hour. An 11% (w/v) PVA solution was prepared by dissolving PVA in distilled water at 80°C with stirring for 6 hours. The COS and PVA solutions were combined in several ratios (1/2, 1/3, 1/4, and 1/5 v/v). The $AgNO_3$ was incorporated into the PVA-COS (2:1) solution at several concentrations (1, 2, 3, 4, 5 wt% to polymer). The synthetic COS-AgNPs (3 wt% to polymer) were added to the PVA solution. All solutions were stirred for 12 hours at room temperature to obtain a homogenous mixture. The conductivity of the electrospinning solutions was determined using an electric conductivity meter (DDS-11A, Shanghai Precision and Scientific Instrument Co, Ltd, Shanghai, People's Republic of China) at 25°C.

Electrospinning

During electrospinning, a high-voltage power source (DW-P303-1ACD8, Guangzhou, People's Republic of China)

was applied to the polymer solution contained in a syringe through an alligator clip attached to the syringe needle (internal diameter 0.9 mm). The applied voltage was adjusted to 15 kV. A syringe pump (TJ-3A, Baoding Longer Precision Pump Co., Ltd, People's Republic of China) was used to control the flow rate (0.5 mL/hour) of the polymer solution. The fibers were collected on electrically grounded aluminum foil placed 10 cm from the needle tip. Subsequently, the PVA/COS/$AgNO_3$ nanofibers were irradiated with ultraviolet light for 8 hours to convert the Ag^+ ions to AgNPs. The PVA/COS-AgNP nanofibers did not require irradiation.

Cross-linking

The PVA/COS/$AgNO_3$ and PVA/COS-AgNP nanofibers were cross-linked in glutaraldehyde vapor at room temperature for several hours, and heated at 80°C for another 4 hours to remove any residual glutaraldehyde.

Physicochemical characterization of nanofibers

Scanning electron microscopy and field emission transmission electron microscopy

The morphology and diameter of the nanofibrous mats were determined via scanning electron microscopy (S-3000N, Hitachi, Tokyo, Japan) and field emission transmission electron microscopy (FE-TEM, Libra 200, Zeiss, Germany). The average diameter of the nanofibers was determined by measuring the diameters of 50 randomly selected fibers.

Mechanical property measurements

The tensile strength of the electrospun nanofibers was tested using a universal testing machine (AI-7000S, Gotech, Taiwan). Test specimens (10 mm wide × 20 mm long) were tested at a crosshead speed of 10 mm per minute and a gauge length of 25 mm under ambient conditions. A minimum of five specimens for each individual scaffold was tested.

Ultraviolet-visible spectroscopy

The ultraviolet-visible spectra of the PVA/CS/$AgNO_3$ and PVA/COS-AgNP electrospinning fiber solutions were recorded using a spectrophotometer (DU-800, Beckman Coulter Inc, Fullerton, CA, USA). The scanning wave ranged from 200–800 nm with an interval of 1.0 nm.

X-ray diffraction

The X-ray diffraction patterns of the electrospinning fibers were obtained using an X-ray diffractometer (D/MAX-2500X, Rigaku, Tokyo, Japan) with Cu Kα characteristic radiation (wavelength λ = 0.154 nm at 40 kV, 150 mA, and a scan speed of 4° per minute in the 2θ range of 5°–80°).

Fourier transform infrared spectroscopy

Fourier transform infrared spectroscopy was performed using a Spectrum PerkinElmer (Wiesbaden, Germany). The infrared spectra of the $AgNO_3$, COS, and COS-AgNP powders and the PVA/COS, PVA/COS/$AgNO_3$ and PVA/COS-AgNP mats were measured over a wavelength range of 4,000–650 cm^{-1}.

Differential scanning calorimetry

The thermal behaviors of the drug, polymer, and electrospun fibers were studied using differential scanning calorimetry (STA-449 C, Netzsch, Selb, Germany). Samples were sealed in aluminum pans and heated from 0°C to 400°C at a heating rate of 10°C per minute.

Water vapor transmission rate

The water vapor permeability rate (WVPR) through the nanofibers was determined as described by Vargas et al using the ASTM E 96 desiccant method.[14] An open cup containing a silica gel desiccant was sealed with the specimen membrane so that the mouth of the cup masked the nonwoven fabric (blank control group, thickness 0.20 mm) or the nonwoven fabric and the test nanofibers stacked in two layers (treatment group, thickness 0.35 mm). The assembly was then placed in a test chamber at 37°C with a constant relative humidity (RH) of 75% for 24 hours. The change in weight of the permeation cup with the specimen was recorded. The water vapor permeability rate was calculated using equation (1) as follows:

$$R_{wvp} = W/(A \times \Delta p) \quad (1)$$

in which R_{WVP} is the WVPR ($g \cdot h^{-1} \cdot cm^{-2} \cdot mmHg^{-1}$), W is the quantity of water vapor permeating the film ($g \cdot h^{-1}$), A is the area of the exposed membrane (2.83 cm^2), and Δp is the vapor pressure difference (mmHg). The permeability P was calculated using equation (2):

$$P = R_{WVP} \times d \quad (2)$$

in which d is the thickness of the membrane.

Degree of swelling and weight loss

The degree of swelling and weight loss from both the neat and the drug-loaded fiber mats was measured after the samples

were submerged in phosphate-buffered solution (pH 7.4) at 37°C for 24 hours, according to the equations (3) and (4):

$$\text{Degree of swelling (\% water uptake)} = \left[\frac{W_t - W_d}{W_d}\right] \times 100 \quad (3)$$

$$\text{Weight loss (\%)} = \frac{W_o - W_d}{W_d} \times 100 \quad (4)$$

in which W_t and W_d are wet and dry weights of the mats after submersion in the buffer solution for 24 hours, respectively, and W_o is the initial weight of the sample in its dry state.

In vitro Ag release

The PVA/CS/$AgNO_3$ and PVA/CS-AgNP electrospinning fibers (approximately 25 mg) were immersed in a 50 mL of acetate buffer (pH 5.5) after cross-linking. The samples were incubated at 37°C and stirred at 100 rpm. Aliquots of each sample (1 mL) were taken from the release medium at specific intervals and diluted to 5 mL with fresh buffer solution to assess the quantity of drug released at various times up to 5 days. The Ag concentration of the solution was determined using an atomic absorption spectrophotometer (Z5000, Hitachi).

Primary skin irritation test

The primary skin irritation test was performed on healthy New Zealand White rabbits (weighing 2–2.5 kg). The rabbits were randomly divided into two groups, ie, a single application group and a multiple application group.[15] The fur was removed from the dorsal surface of the rabbits 24 hours prior to administration, and the injury model was obtained by scarifying intact skin until capillary hemorrhage with an area of 3 cm × 3 cm. For the irritation test, the dorsal skin of each rabbit was divided into four regions for the application of the PVA/COS/$AgNO_3$ nanofiber product, the PVA/CS-AgNP nanofiber product, gauze, and no treatment. For the single application group, the preparations were applied to the corresponding region, and the animals were examined for signs of irritation at approximately one, 24, 48, and 72 hours after application.[16] For the multiple application group, the preparations were applied on the same skin regions for 24 hours. The application sites were assessed 1 hour after removing the preparation, and this procedure was repeated for another 3 days. After the final removal, the multiple administration group was monitored for 72 hours. Mean erythema and edema scores were recorded according to the Draize method,[17] ie, for erythema and eschar formation (no erythema = 0; very slight erythema = 1; well-defined erythema = 2; moderate to severe erythema = 3; severe erythema and slight eschar formation = 4), and edema formation (no edema = 0; very slight edema = 1; slight edema = 2; moderate edema = 3; severe edema = 4).

Cytotoxicity evaluation

The potential cytotoxicity of the nanofibers was evaluated against human skin fibroblasts. The PVA/COS/$AgNO_3$ and PVA/COS-AgNP nanofibers were sterilized under ultraviolet light for 1 hour on each side, then immersed in serum-free medium containing only Dulbecco's Modified Eagle's Medium and placed in an incubator for 24 hours to produce extraction media of 0.2, 0.4, 0.8, and 1.0 mg/mL. The supernatant was then filtered through a 0.22 μm Millipore membrane (Millipore, Billerica, MA, USA). Fresh Dulbecco's Modified Eagle's Medium supplemented with 10% fetal bovine serum was used as a negative control. The human skin fibroblasts were plated in 90 μL of Dulbecco's Modified Eagle's Medium supplemented with 10% fetal bovine serum at a density of 1×10^5 cells/well in 96-well plates, and the cells were cultured at 37°C in a wet atmosphere containing 5% CO_2. Twenty-four hours after plating, the extraction medium containing 10% fetal bovine serum was replaced, and the cells were incubated for an additional 24 hours. The tested extraction solutions were then removed. Finally, the cells were incubated in 100 μL of MTT-containing medium (1 mg/mL) for 4 hours. After the medium was removed, the formazan crystals formed in the living cells were dissolved in 100 μL of dimethylsulfoxide. Cell viability (%) was calculated based on the absorbance at 490 nm using a microplate reader (353-MK3, Thermo Labsystems, Franklin, MA, USA).

Antibacterial assessment

Zone of inhibition

Escherichia coli and *Staphylococcus aureus* were used as test organisms for the zone of inhibition test. A bacterial solution (100 μL, with a concentration of ~10^6 colony-forming units per mL) was dispensed onto an agar plate, and neat PVA/COS (2:1), PVA/COS/$AgNO_3$ (3%), and PVA/COS-AgNP nanofibers (1.5 cm × 1.5 cm) were placed on the surface of the plate. The zone of inhibition was measured after 24 hours of incubation at 37°C.

Antibacterial kinetic testing

Approximately 15 mg of neat PVA/COS (2:1), non-treated PVA/COS/3% $AgNO_3$, PVA/COS with varying concentrations of $AgNO_3$ (1%, 3%, and 5%), and PVA/

COS-AgNP nanofibers were added into 50 mL of bacteria nutrient solution with a bacterial concentration of ~10^4 colony-forming units per mL). A bacteria nutrient solution with the same concentration was used as the control. The optical density of the bacterial broth at 600 nm was measured by ultraviolet-visible spectrophotometry.[18] The inhibition ratios of the fibers were calculated using equation (5):

$$\text{Inhibition ratio } (\%) = 100 - 100 \times \frac{A_t - A_o}{A_{con} - A_o}, \quad (5)$$

in which A_0 is the optical density of the bacterial broth medium prior to incubation, and A_t and A_{con} are the optical densities of the bacterial solutions after incubating the fibers and control sample for the desired interval, respectively.

Wound healing test

Twelve Sprague Dawley rats (200–250 g) were used in this study, which was approved by the ethical committee of the Experimental Animal Centre of the Third Military Medical University. After anesthetization, a 5 cm × 4 cm area on the dorsal side of the rats was shaved. Four full-thickness circular wounds with a surface area of 2.25 cm^2 were created on the back of each rat. Each wound was covered with the test samples. Group 1 wounds were treated with PVA/COS/$AgNO_3$ nanofibers, group 2 wounds were treated with PVA/COS-AgNP nanofibers, group 3 wounds were covered with gauze as a blank treatment, and group 4 wounds were treated with woundplast (Yunnan Baiyao Group Co, Ltd, Jiangchuan, People's Republic of China) as a control. The area of the wound was measured using the planimetry method at one, 3, 7, 10 and 14 days after injury. The percentage healing is defined by equation (6):

$$\text{Wound area } (\%) = AT/AO \times 100 \quad (6)$$

in which AO is the initial wound area and AT is the measured area. In addition, the wounded skin was removed at 7 and 14 days after injury for histopathological observation of epithelialization and granulation.

Statistical analysis

The statistical analyses were performed using Statistical Package for the Social Sciences version 18 software (SPSS Inc., Chicago, IL, USA). All data are expressed as the mean ± standard deviation. For comparisons among groups, one-way analysis of variance with post hoc Bonferroni tests were performed. Differences were considered statistically significant at $P<0.05$.

Results and discussion

Electrospinning

Conductivity is an important parameter during the electrospinning process. Table 1 shows the effect of the PVA mass ratio and COS and $AgNO_3$ concentrations on the conductivity of the electrospinning solutions. The conductivity clearly decreased as the mass ratio of PVA and COS increased, but was not significantly altered by $AgNO_3$ concentration.

Figure 1A shows scanning electron microscopic images of the PVA/COS (2:1), PVA/COS/3%$AgNO_3$, and PVA/COS-AgNP fiber mats, indicating smooth fibers with diameters of 192.57 ± 59.30 nm, 159.43 ± 40.35 nm, and 130.13 ± 43.55 nm, respectively (Figure 1B), without beads. The decrease in diameter of the nanofibers is largely due to the conductivity of the solution (Table 1). When the conductivity of a solution increases, the diameter of the nanofiber decreases.[5] Solutions with high conductivity will have greater charge-carrying capacities; with the aid of high charge density, high elongation forces are then imposed upon the jet, resulting in a reduction in diameter.[2,18]

Figure 1C shows FE-TEM micrographs of non-ultraviolet-treated PVA/COS/3% $AgNO_3$, post-ultraviolet-treated PVA/COS/3% $AgNO_3$, and PVA/COS-AgNP fiber mats. The AgNPs were spherically dispersed on the surface of the fibers. A higher AgNP density was observed in the post-ultraviolet-treated PVA/COS/3% $AgNO_3$ and PVA/COS-AgNP nanofibers. The diameters of the AgNPs in the PVA/COS-AgNP and PVA/COS/3%$AgNO_3$ nanofibers were 15.70 ± 4.73 nm and 22.26 ± 7.00 nm, respectively.

The tensile strengths of PVA/COS/3%$AgNO_3$ and PVA/COS-AgNP fiber mats were 9.90 ± 1.83 MPa and 15.21 ± 1.86 MPa, respectively, with the latter nanofiber showing better tensile strength. These results indicate that the mechanical properties of the nanofiber membranes are

Table 1 Conductivity of the PVA/COS solutions

Components	Conductivity (mS cm^{-1})
PVA:COS = 2:1	2.43 ± 0.04
PVA:COS = 3:1	1.89 ± 0.03
PVA:COS = 4:1	1.79 ± 0.04
PVA:COS = 5:1	1.45 ± 0.08
PVA:COS:1% $AgNO_3$	2.73 ± 0.09
PVA:COS:2% $AgNO_3$	2.76 ± 0.02
PVA:COS:3% $AgNO_3$	2.80 ± 0.06
PVA:COS:4% $AgNO_3$	2.72 ± 0.03
PVA:COS:5% $AgNO_3$	2.71 ± 0.08
PVA:COS-AgNPs	3.21 ± 0.14

Abbreviations: AgNPs, silver nanoparticles; COS, chitosan oligosaccharide; PVA, poly(vinyl alcohol).

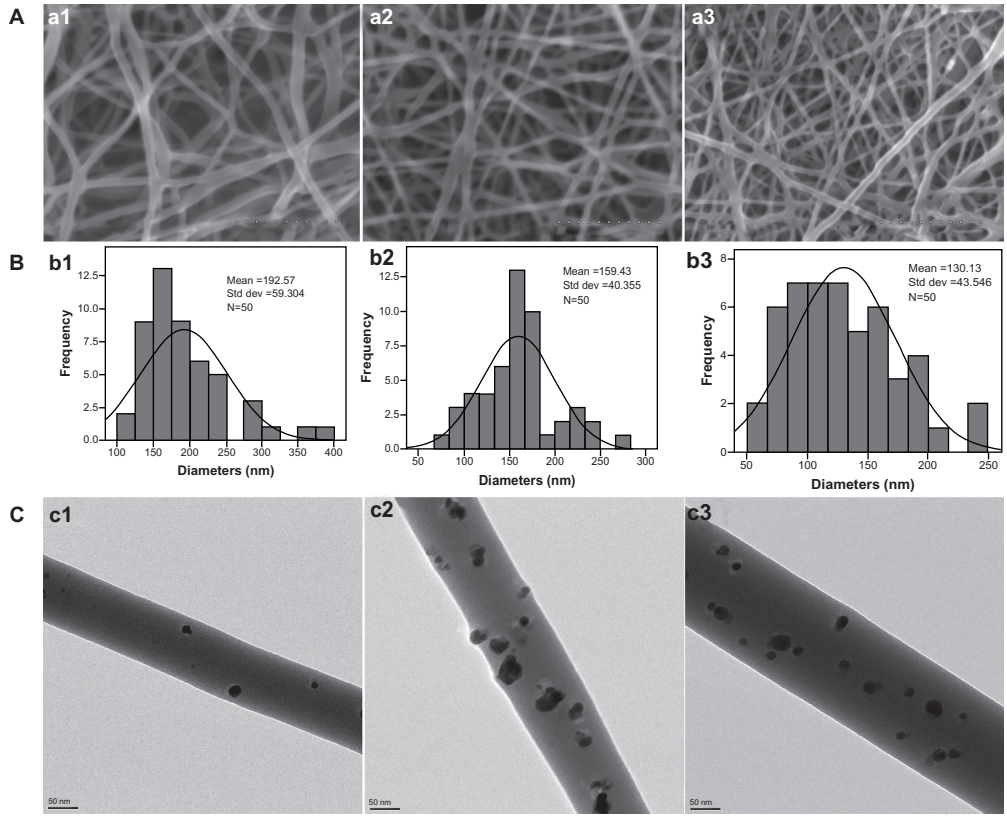

Figure 1 (**A**) Scanning electron micrographs of (**a1**) the neat PVA/COS nanofiber, (**a2**) the PVA/COS/3% $AgNO_3$ nanofiber, and (**a3**) the PVA/COS-AgNP nanofiber. (**B**) Diameter distribution of (**b1**) the neat PVA/COS nanofiber, (**b2**) the PVA/COS/3% $AgNO_3$ nanofiber and (**b3**) the PVA/COS-AgNPs nanofiber. (**C**) Field emission transmission electron micrographs of (**c1**) the non-UV-treated PVA/COS/3% $AgNO_3$ nanofiber (**c2**) the post-UV-treated PVA/COS/3% $AgNO_3$ nanofiber, and (**c3**) the PVA/COS-AgNP nanofiber.

Abbreviations: AgNP, silver nanoparticle; COS, chitosan oligosaccharide; PVA, poly(vinyl alcohol); UV, ultraviolet; Std dev, standard deviation.

sufficient for practical handling during the wound healing process.

Formation of AgNPs in the electrospinning solution was detected by ultraviolet-visible spectroscopy. The ultraviolet-visible spectra of the different nanofiber solutions are shown in Figure 2. For the COS-AgNP, PVA/COS/$AgNO_3$, and PVA/COS-AgNP fiber mats, maximum absorption was observed at approximately 405 nm, which is a typical surface plasmon absorption for AgNPs.[19] The non-ultraviolet-treated PVA/COS/$AgNO_3$ mats showed a slight absorption band, likely due to the small quantities of AgNPs generated by light during the electrospinning process.

X-ray diffraction

The X-ray diffraction pattern of the PVA/COS-AgNP mat (Figure 3B) showed clear peaks at approximately 38.3 and 44.2, corresponding to the crystal (111) and (200) planes, respectively, of the standard Ag cubic phases.[20] Similar peaks were observed for the PVA/COS/$AgNO_3$ mat (Figure 3A) but at lower intensities, which can be attributed to the low AgNP content.

Fourier transform infrared spectroscopy

The Fourier transform infrared spectra for the PVA/COS, PVA/COS/$AgNO_3$, and PVA/COS-AgNP nanofibers are shown in Figure 4. The characteristic peaks of the neat PVA/COS nanofibers were assigned as follows: 3,308 cm^{-1} (N-H group), 2,942 cm^{-1} (CH_2 asymmetric vibration), and 1,715 and 1,085 cm^{-1} (C=O bond). The peak at 1,248 cm^{-1} was associated with C=O=C vibrations and indicates the cross-linking of some PVA radicals.[21] For the PVA/COS and PVA/COS/$AgNO_3$ mats, the two spectra were similar with no shifts in any of the peaks, suggesting that the AgNPs were physically entrapped in the scaffold by van der Waals forces. Similar results have been reported by others.[22,23] A significant change in the shape of the band at 3,338 cm^{-1} was observed between the PVA/COS nanofibers and the PVA/COS-AgNP nanofibers, indicating that N-H vibration was affected by attachment of the AgNPs.

Differential scanning calorimetry

Figure 5 shows the differential scanning calorimetry thermograms for PVA, PVA/COS, PVA/COS/$AgNO_3$, and

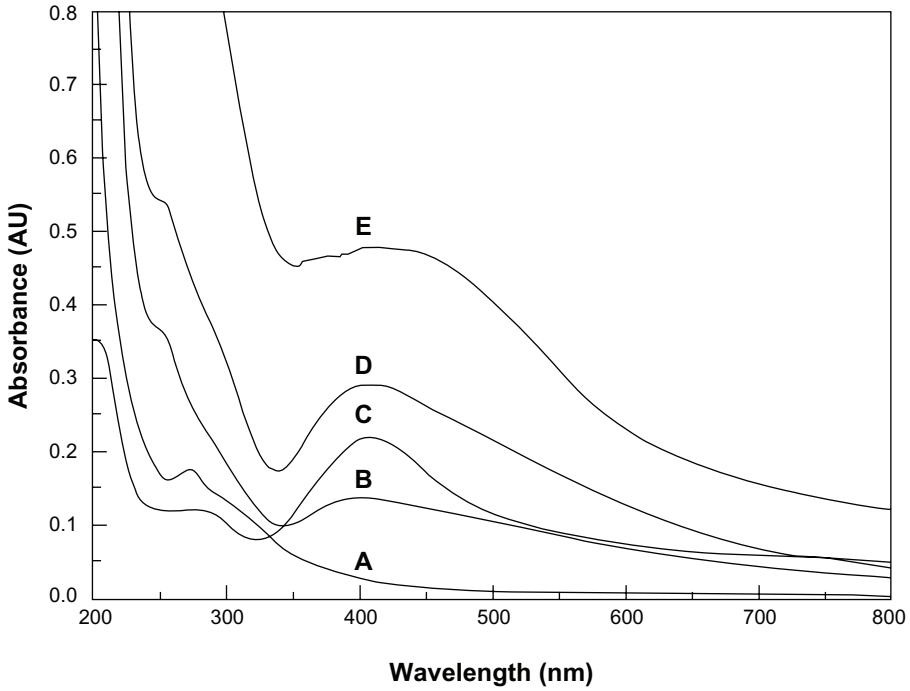

Figure 2 Ultraviolet-visible spectra for the nanofiber aqueous solutions. (**A**) The neat PVA/COS nanofiber, (**B**) the non-ultraviolet-treated PVA/COS/$AgNO_3$ nanofiber, (**C**) the PVA/COS/$AgNO_3$ nanofiber, (**D**) the PVA/COS-AgNP nanofiber, and (**E**) COS-AgNPs.
Abbreviations: AgNP, silver nanoparticle; COS, chitosan oligosaccharide; PVA, poly(vinyl alcohol); AU, absorbance units.

PVA/COS-AgNP nanofibers. The melting points (T_ms) of the PVA and PVA/COS nanofibers were observed at 188.2°C and 184.5°C, respectively. The T_ms of the PVA/COS/$AgNO_3$ and PVA/COS-AgNP nanofibers were observed at 180.6°C and 189.4°C, respectively.

Water vapor permeability

Wound dressings require permeability of moisture and gases through the film to keep the wound comfortable and aid in the healing process.[14] Figure 6A shows the water vapor permeability of the PVA/COS (2:1) mats cross-linked by glutaraldehyde vapor at various intervals. The nanofibers did not exhibit any statistically significant difference ($P<0.05$) in water vapor permeability measured within 48 hours, but were significantly reduced after 72 hours. As the volume ratio of the PVA/COS increased, the water vapor permeability decreased (Figure 6B). No significant difference in water vapor permeability was noted between the PVA/COS/$AgNO_3$ and PVA/COS-AgNP mats.

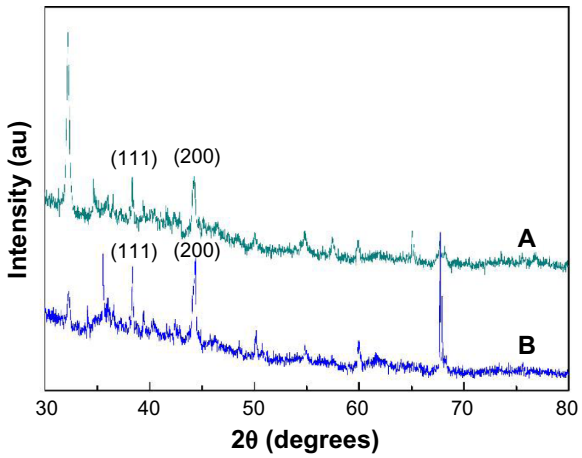

Figure 3 X-ray diffraction curves for (**A**) the PVA/COS/$AgNO_3$ nanofiber and (**B**) the PVA/COS-AgNP nanofiber.
Abbreviations: AgNP, silver nanoparticle; COS, chitosan oligosaccharide; PVA, poly(vinyl alcohol).

Swelling and weight loss of the neat and drug-loaded fiber mats

Figure 7A shows the degree of swelling and weight loss for the nanofibers cross-linked by glutaraldehyde vapor at various intervals after immersion in a pH 7.4 phosphate-buffered solution at 37°C. The high degree of swelling observed at shorter cross-linking intervals was due to the large quantity of water absorbed by the highly porous membrane. As the cross-linked time increased, the degree of swelling and amount of weight loss both decreased.

When the cross-linking time was fixed at 48 hours, the volume ratio of the PVA and COS increased, and the degree of swelling and weight loss decreased slightly.

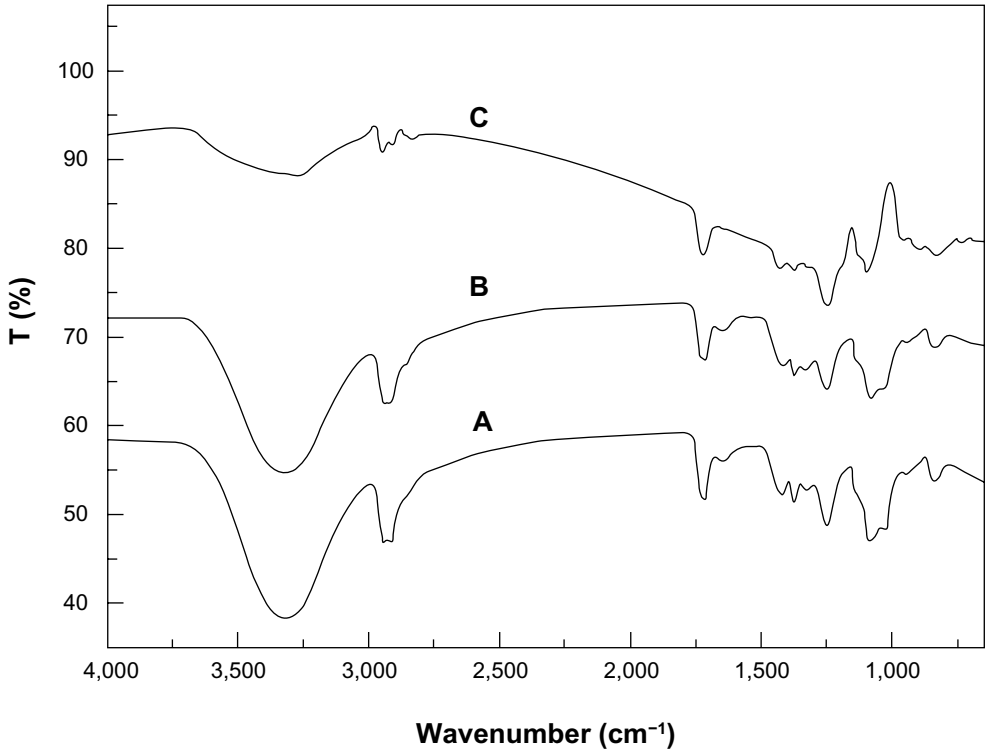

Figure 4 Fourier transform infrared spectra of (**A**) the neat PVA/COS nanofiber, (**B**) the PVA/COS/$AgNO_3$ nanofiber, and (**C**) the PVA/COS-AgNP nanofiber.
Abbreviations: AgNP, silver nanoparticle; COS, chitosan oligosaccharide; PVA, poly(vinyl alcohol).

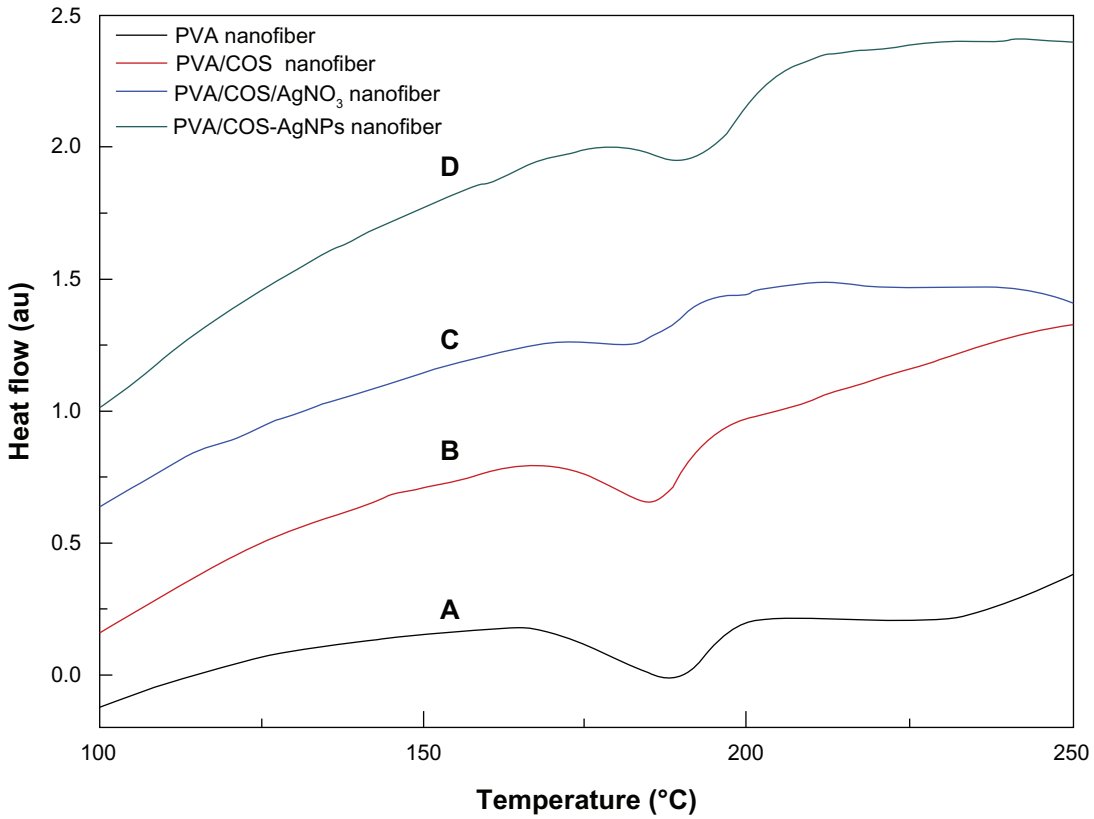

Figure 5 Differential scanning calorimetric thermograms for the (**A**) PVA nanofiber, (**B**) the neat PVA/COS nanofiber, (**C**) the PVA/COS/$AgNO_3$ nanofiber, and (**D**) the PVA/COS-AgNP nanofiber.
Abbreviations: AgNP, silver nanoparticle; COS, chitosan oligosaccharide; PVA, poly(vinyl alcohol); au, arbitrary units.

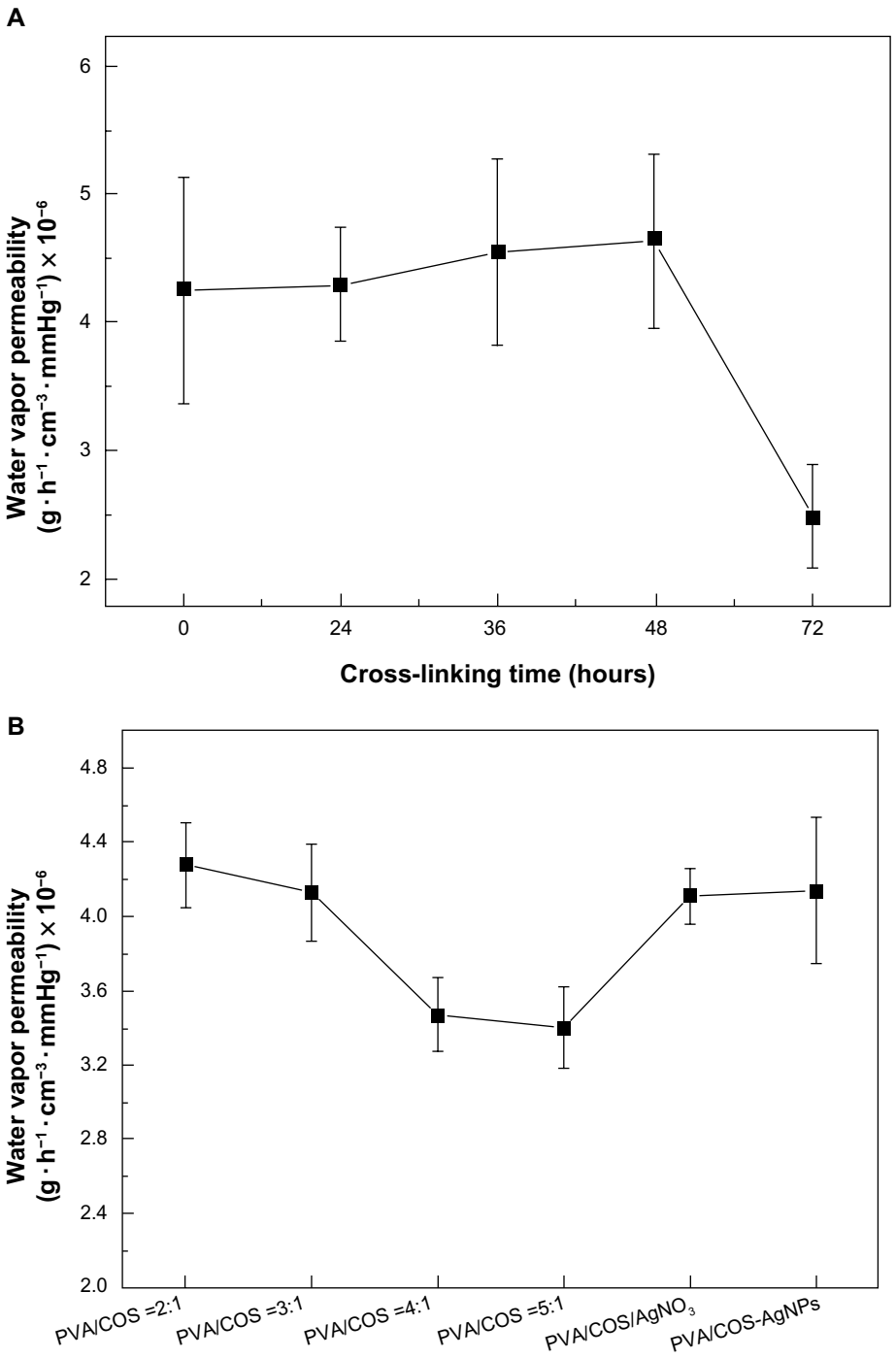

Figure 6 Water vapor permeability of (**A**) the PVA/COS nanofibers with a volume ratio of 2:1 cross-linked by glutaraldehyde vapor at various intervals and (**B**) the neat and drug-loaded nanofibers.
Abbreviations: AgNP, silver nanoparticle; COS, chitosan oligosaccharide; PVA, poly(vinyl alcohol).

Two drug-loaded fiber mats showed reduced weight loss and slightly increased swelling compared with the neat electrospun fiber mat (Figure 7B). Electrospun PVA/COS-AgNPs showed less weight loss than electrospun PVA/COS/$AgNO_3$, with no statistically significant difference ($P>0.05$) in the degree of swelling.

An ideal wound dressing should be permeable to maintain a moist environment and prevent dehydration.[24] Therefore, it should have high permeability, a high degree of swelling, and little weight loss. Generally, we found that cross-linking with glutaraldehyde vapor for 48 hours and a PVA:COS volume ratio of 2:1 produced optimal nanofibers.

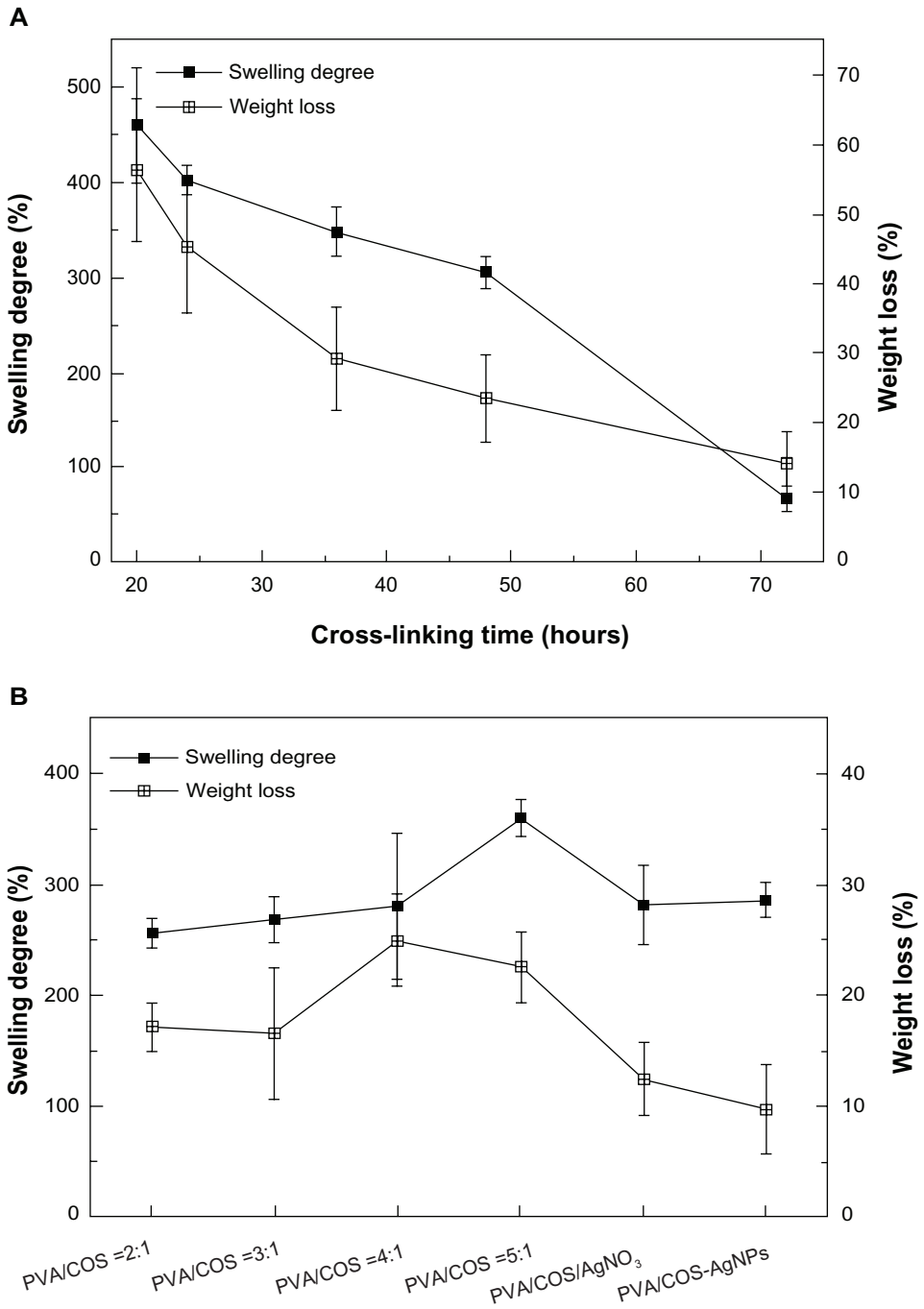

Figure 7 Degree of swelling and weight loss from (**A**) the PVA/COS nanofibers with a volume ratio of 2:1 cross-linked with glutaraldehyde vapor at various intervals and (**B**) the neat and drug-loaded nanofibers.
Abbreviations: AgNP, silver nanoparticle; COS, chitosan oligosaccharide; PVA, poly(vinyl alcohol).

Silver loading and in vitro release study

To determine the quantity of Ag that was actually present in the COS-AgNP sample, 5 mg of the sample was dissolved in 10 mL of 50% nitric acid (HNO_3), allowed to digest for 2 hours, and diluted to 100 mL using double-distilled water as a releasing medium. The Ag-containing solution obtained was subjected to atomic absorption spectroscopy, and the actual content of Ag in the nanoparticles was found to be 0.143 g/100 mL.

The release characteristics for the model drugs from the cross-linked PVA/COS-AgNP and the PVA/COS/$AgNO_3$ nanofibers were determined using the total immersion method with acetate buffer (pH 5.5) as the transferring medium at 37°C. The cumulative release of the drug from

the drug-loaded fiber mats as a function of immersion time is shown in Figure 8. Release of Ag from both samples was rapid during the first 8 hours after immersion in the releasing medium and increased gradually thereafter. The maximum release of Ag from the PVA/COS-AgNP fiber mat exceeded the quantity released from the PVA/COS/$AgNO_3$ fiber mat. Therefore, the PVA/COS-AgNP fiber mat released Ag into the acetate buffer more readily than the PVA/COS/$AgNO_3$. This rapid and constant release of Ag from the fiber web could provide more rapid and constant antimicrobial activity at the wound site.

Indirect cytotoxicity evaluation

The cytotoxicity of various concentrations of the extraction medium from the neat PVA/COS, PVA/COS/$AgNO_3$, and PVA/COS-AgNP nanofiber mats is shown in Figure 9. Cell viability decreased significantly when human skin fibroblasts were incubated with higher concentrations (0.8–1.0 mg/mL) of the extraction medium from the PVA/COS/$AgNO_3$ nanofiber mat when compared with the control ($P<0.05$). However, no significant cytotoxicity was observed at any concentration with the neat PVA/COS and PVA/COS-AgNP nanofiber mats. These data suggest that the PVA/COS-AgNP nanofiber mat has excellent in vitro biocompatibility and has marked benefits over the PVA/COS/$AgNO_3$ nanofiber mat at the concentrations tested (0.8–1.0 mg/mL).

Skin irritation test

The results of the skin irritation test for single and multiple applications are shown in Tables 2 and 3, respectively. According to the intensity criteria for skin irritation, scores below 0.5 were regarded as indicating no irritation. As shown in Tables 2 and 3, both PVA/COS/$AgNO_3$ and PVA/COS-AgNP nanofiber mats caused no irritation to normal skin after single and multiple applications, indicating the acceptability of these nanofibers for transdermal drug delivery.

Antibacterial assessment

The antibacterial properties of the nanofibers were explored in *S. aureus* and *E. coli* by measuring bacterial growth inhibition halos and by bactericidal kinetic testing. Figure 10 shows the antibacterial activity of the neat PVA/COS, PVA/COS/$AgNO_3$, and PVA/COS-AgNP nanofibers using a zone inhibition test. In these experiments, no zones of inhibition were observed for the neat PVA/COS nanofiber. As shown in Figure 9B–F, PVA/COS/$AgNO_3$ and PVA/COS-AgNP nanofibers displayed high antibacterial activity against both *S. aureus* and *E. coli*. The size of the zone of inhibition increased slightly for the PVA/COS-AgNP nanofiber.

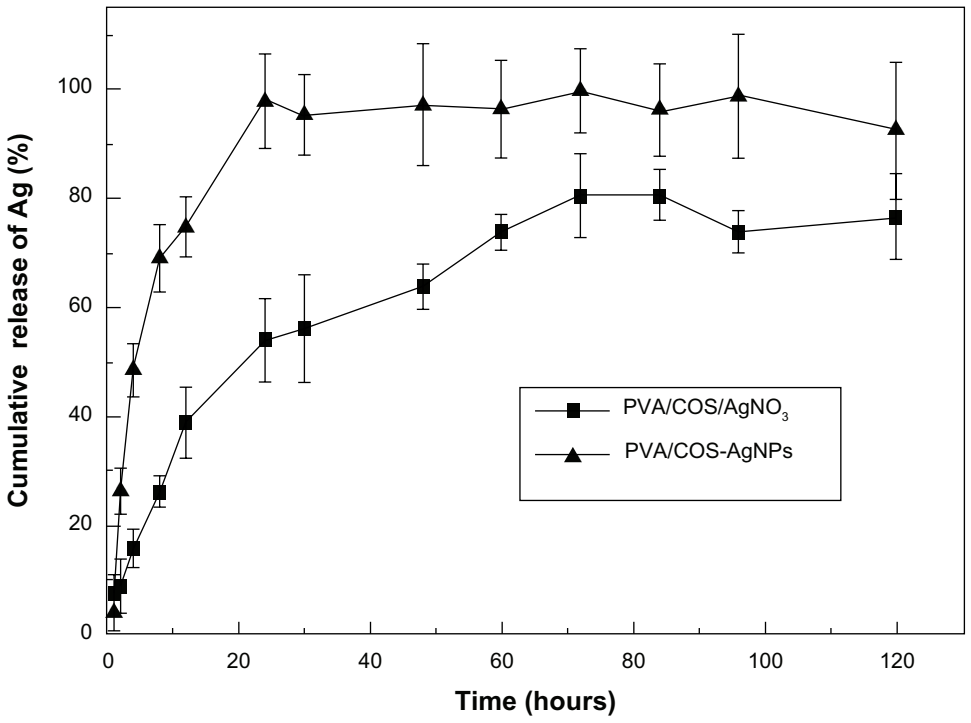

Figure 8 In vitro Ag release profiles from the PVA/COS-AgNP nanofiber and the PVA/COS/$AgNO_3$ nanofiber.
Abbreviations: AgNP, silver nanoparticle; COS, chitosan oligosaccharide; PVA, poly(vinyl alcohol).

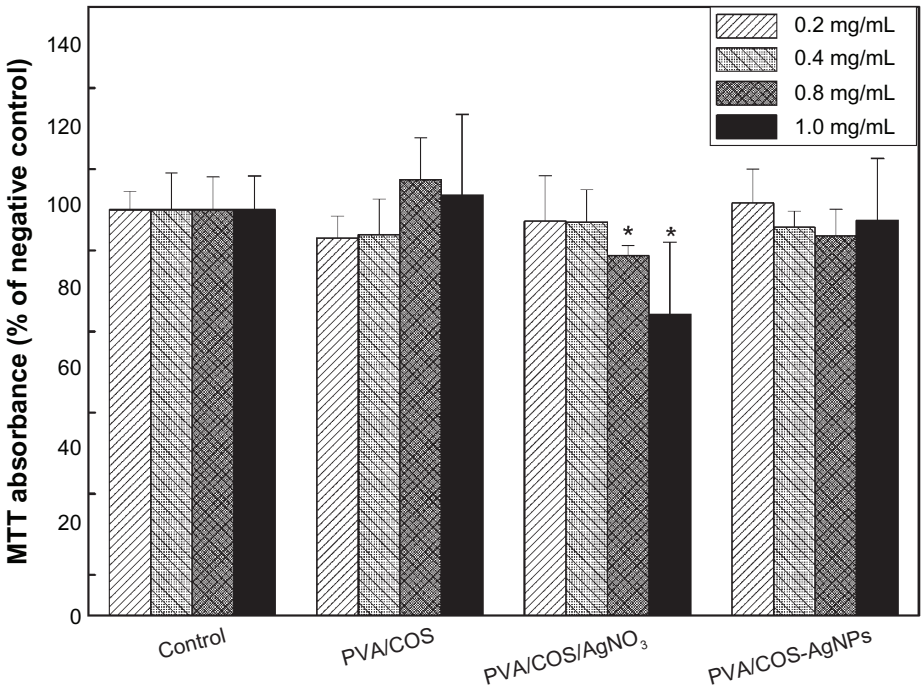

Figure 9 Cytotoxicity tests from the MTT assays of cell viability. Absorbance was normalized to that of the negative control at each time interval, and was considered 100%.
Notes: *$P<0.05$ compared with the negative control. The data are presented as the mean ± standard deviation (n=5).
Abbreviations: AgNP, silver nanoparticle; COS, chitosan oligosaccharide; PVA, poly(vinyl alcohol).

Figure 11 shows the bactericidal kinetic testing results for the various nanofibers. The neat PVA/COS nanofiber displayed slight antibacterial activity at 12 hours. The AgNP-decorated PVA/COS nanofibers demonstrated excellent bactericidal efficiency toward both microorganisms. As the quantity of $AgNO_3$ increased, the inhibition ratio expanded. The PVA/COS-AgNP mat (average AgNP diameter 15 nm) showed more effective antibacterial activity than the PVA/COS/$AgNO_3$ mat (average AgNP diameter 22 nm) against both microorganisms, a difference that may be due to the release rates for Ag^+ ions or AgNPs,[6] and the sizes of the AgNPs.[25] The larger surface area of the smaller AgNPs provided a larger area for bacteria interaction, enhancing their antibacterial effect.[10,26,27] Thus, the AgNP-containing nanofibers are advantageous as antibacterial materials.

Wound healing and histological examination

To assess wound healing, four full-thickness circular wounds were cut into the back of each rat, and the wounds were covered with PVA/COS/$AgNO_3$, PVA/COS-AgNP nanofiber mats, commercially available woundplasts (positive control), or gauze (negative control). Figure 12 shows the animals from each group at one, 7, and 14 days after grafting. Wound closure was observed in all treatment groups within 14 days. The grafts prepared with nanofiber scaffolds were well integrated into the surrounding skin. The wound areas decreased

Table 2 Average primary skin irritation index values for single application (n=4)

Samples	Average score			
	1 hour	24 hours	48 hours	72 hours
PVA/COS/$AgNO_3$ nanofiber mat	0.05 ± 0.10	0.00 ± 0.00	0 ± 0.00	0 ± 0.00
PVA/COS-AgNP nanofiber mat	0.28 ± 0.19	0.18 ± 0.13	0.05 ± 0.10	0 ± 0.00
Gauze	0.16 ± 0.21	0.10 ± 0.20	0 ± 0.00	0 ± 0.00

Abbreviations: AgNP, silver nanoparticle; COS, chitosan oligosaccharide; PVA, poly(vinyl alcohol).

Table 3 Average primary skin irritation index values for multiple applications (n=4)

Samples	Average score			
	1 hour	24 hours	48 hours	72 hours
PVA/COS/$AgNO_3$ nanofiber mat	0.10 ± 0.12	0.13 ± 0.15	0.08 ± 0.15	0.05 ± 0.10
PVA/COS-AgNP nanofiber mat	0.03 ± 0.05	0.05 ± 0.10	0.05 ± 0.10*	0.03 ± 0.05
Gauze	0.10 ± 0.14	0.18 ± 0.13	0.23 ± 0.05	0.10 ± 0.08

Note: *$P<0.05$ compared with gauze.
Abbreviations: AgNP, silver nanoparticle; COS, chitosan oligosaccharide; PVA, poly(vinyl alcohol).

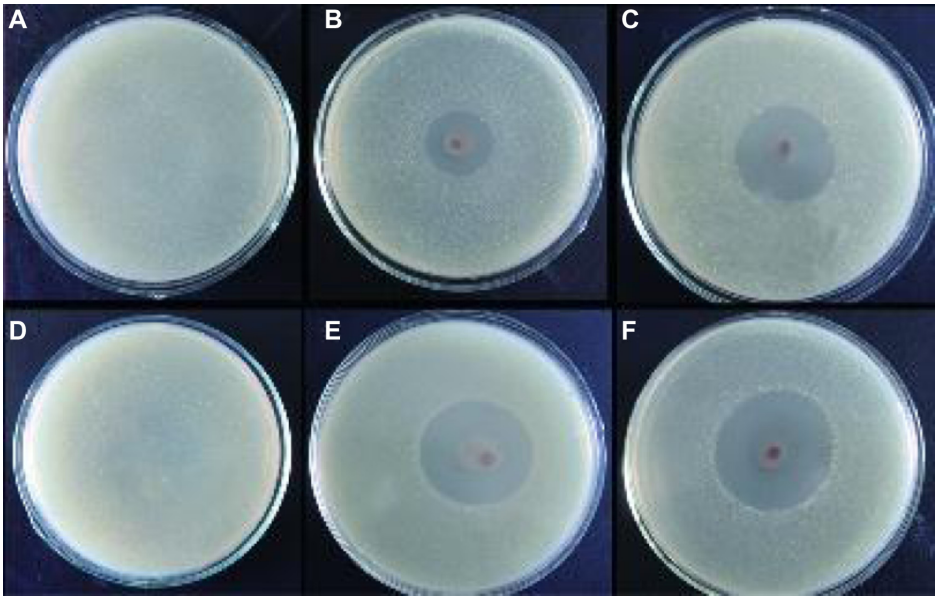

Figure 10 Zone of inhibition test for (**A** and **D**) the neat PVA/COS nanofiber (**B** and **E**) the PVA/COS/$AgNO_3$ nanofiber, and (**C** and **F**) the PVA/COS-AgNP nanofiber. Also shown are photographs of the disk sensitivity test for *Staphylococcus aureus* (**A**–**C**) and *Escherichia coli* (**D**–**F**).
Abbreviations: AgNP, silver nanoparticle; COS, chitosan oligosaccharide; PVA, poly(vinyl alcohol).

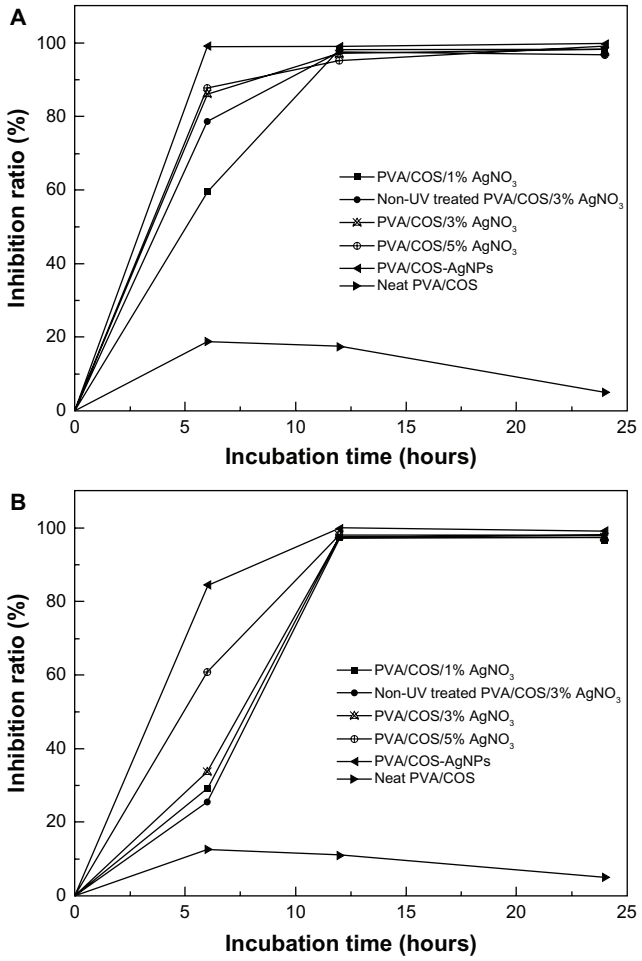

Figure 11 Bactericidal kinetic study against *Staphylococcus aureus* (**A**) and *Escherichia coli* (**B**) for the different nanofibers.
Abbreviations: AgNP, silver nanoparticle; COS, chitosan oligosaccharide; PVA, poly(vinyl alcohol); UV, ultraviolet.

gradually, reaching approximately 3% at 14 days after treatment with the four different wound dressings. Figure 13 shows the changes in wound area at the different healing times. During the first 7 days, the PVA/COS-AgNP nanofiber mats enabled better wound healing than the gauze ($P<0.05$), and produced results similar to those for the PVA/COS/$AgNO_3$ nanofiber mats and the commercial woundplasts. However, the difference between the PVA/COS/$AgNO_3$ nanofiber mats and gauze was not statistically significant. A possible cause for this difference may be the rapid and constant release of AgNPs and the excellent antibacterial capacity of PVA/COS-AgNP nanofibers. The wound area percentages for all treatments between day 9 and recovery were similar.

According to the histological examination shown in Figure 14, the PVA/COS-AgNP nanofiber demonstrated superior wound healing compared with gauze and the PVA/COS/$AgNO_3$ nanofiber. Seven days after grafting, the wounds in the PVA/COS/$AgNO_3$ nanofiber and gauze groups displayed ulcerated surfaces, formation of granulation tissue, and infiltration of inflammatory cells. In contrast, the granulated tissue in the PVA/COS-AgNP group disappeared without capillary hyperplasia. Late-stage healing processes in the control group were similar to those in the AgNP-containing nanofiber groups. On day 14, newly synthesized fibrous tissue and sparse inflammatory cells in the dermis and subcutis were covered by completely re-epithelialized epidermis in each group. These data further confirm that the PVA/COS-AgNP nanofibrous membrane could provide a suitable scaffold for wound healing.

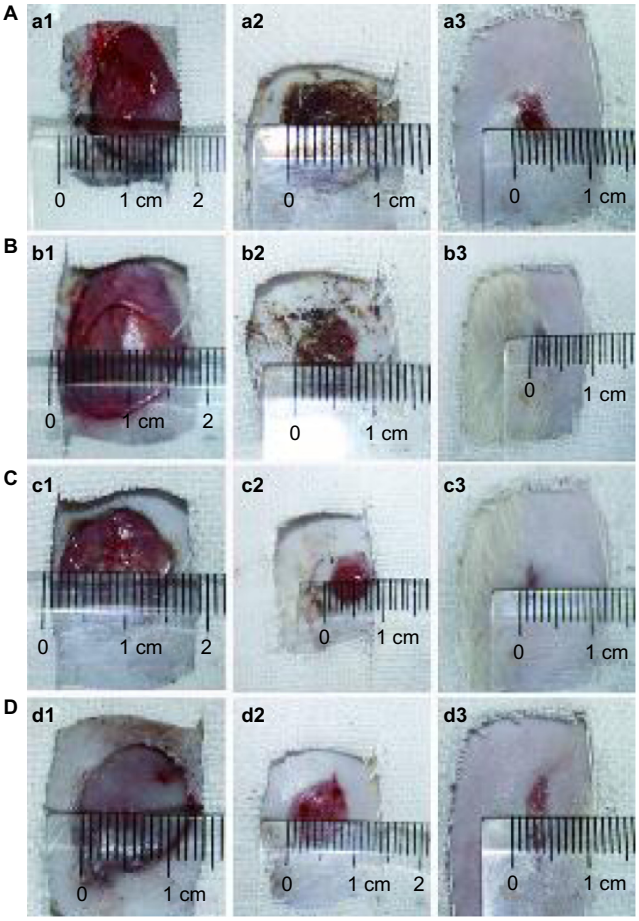

Figure 12 Wound appearance at 1, 7 and 14 days after grafting with (**A**) gauze, (**B**) the PVA/COS/$AgNO_3$ nanofiber, (**C**) the PVA/COS-AgNP nanofiber, and (**D**) the commercial woundplast.
Abbreviations: AgNP, silver nanoparticle; COS, chitosan oligosaccharide; PVA, poly(vinyl alcohol).

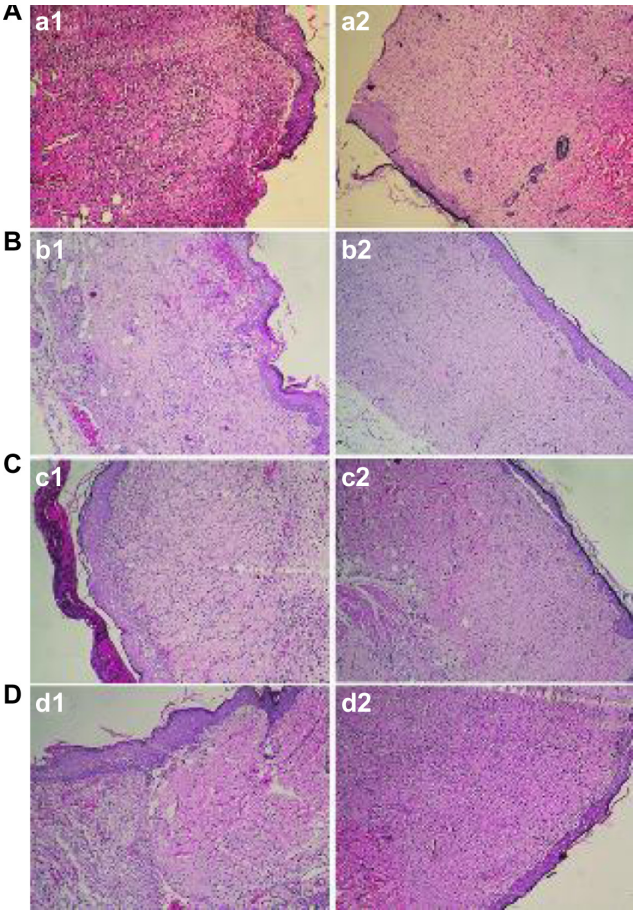

Figure 14 Histological examination after wounds had been covered for 7 and 14 days with (**A**) gauze, (**B**) the PVA/COS/$AgNO_3$ nanofiber, (**C**) the PVA/COS-AgNP nanofiber, and (**D**) the commercial woundplast.
Abbreviations: AgNP, silver nanoparticle; COS, chitosan oligosaccharide; PVA, poly(vinyl alcohol).

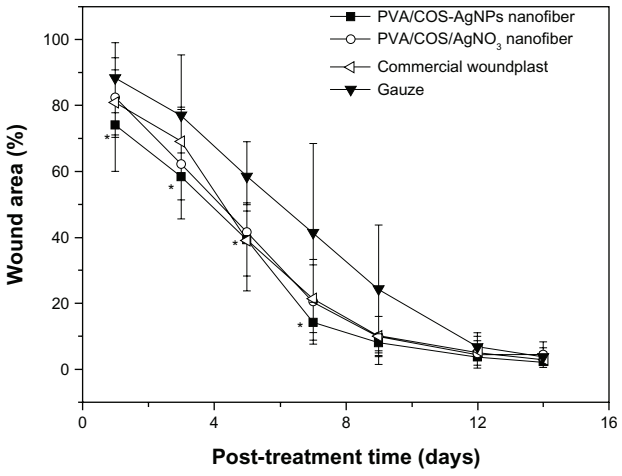

Figure 13 Wound healing with the PVA/COS/$AgNO_3$ nanofiber, the PVA/COS-AgNP nanofiber, commercial woundplast, and gauze.
Notes: *$P<0.05$ compared with the gauze. The data are presented as the mean ± standard deviation (n=6).
Abbreviations: AgNP, silver nanoparticle; COS, chitosan oligosaccharide; PVA, poly(vinyl alcohol).

Conclusion

In the present study, AgNPs (15 nm average diameter) were successfully prepared using a green method. Nonwoven mats of PVA/COS/$AgNO_3$ blends and PVA/COS-AgNP blends were fabricated by electrospinning. The presence of AgNPs was confirmed via scanning electron microscopy, FE-TEM, X-ray diffraction, Fourier transform infrared spectroscopy, and differential scanning calorimetry. The PVA/COS-AgNP nanofiber mats were in the nanometer range, were nontoxic and biocompatible, and displayed sustained-release characteristics, demonstrating excellent antimicrobial activity against Gram-positive *S. aureus* and Gram-negative *E. coli*. Moreover, the PVA/COS-AgNP nanofiber mats accelerated the early stages of wound healing compared with the PVA/COS/$AgNO_3$ nanofiber mats, suggesting that these materials have great potential for use as wound dressings.

Acknowledgment

We gratefully acknowledge the financial support received from the Chongqing Programs for Science and Technology Development (CSTC2012 gg-yyjs10031).

Disclosure

The authors report no conflicts of interest in this work.

References

1. Kumar PT, Lakshmanan V-K, Biswas R, Nair SV, Jayakumar R. Synthesis and biological evaluation of chitin hydrogel/nano ZnO composite bandage as antibacterial wound dressing. *J Biomed Nanotechnol*. 2012;8(6):891–900.
2. Sill TJ, von Recum HA. Electrospinning: applications in drug delivery and tissue engineering. *Biomaterials*. 2008;29(13):1989–2006.
3. Rho KS, Jeong L, Lee G, et al. Electrospinning of collagen nanofibers: effects on the behavior of normal human keratinocytes and early-stage wound healing. *Biomaterials*. 2006;27(8):1452–1461.
4. Chong EJ, Phan TT, Lim IJ, et al. Evaluation of electrospun PCL/gelatin nanofibrous scaffold for wound healing and layered dermal reconstitution. *Acta Biomater*. 2007;3(3):321–330.
5. Charernsriwilaiwat N, Opanasopit P, Rojanarata T, Ngawhirunpat T. Lysozyme-loaded, electrospun chitosan-based nanofiber mats for wound healing. *Int J Pharm*. 2012;427(2):379–384.
6. Cencetti C, Bellini D, Pavesio A, et al. Preparation and characterization of antimicrobial wound dressings based on silver, gellan, PVA and borax. *Carbohydr Polym*. 2012;90(3):1362–1370.
7. Nitanan T, Akkaramongkolporn P, Rojanarata T, Ngawhirunpat T, Opanasopit P. Neomycin-loaded poly (styrene sulfonic acid-co-maleic acid)(PSSA-MA)/polyvinyl alcohol (PVA) ion exchange nanofibers for wound dressing materials. *Int J Pharm*. 2013;448(1):71–78.
8. Kim S-K, Rajapakse N. Enzymatic production and biological activities of chitosan oligosaccharides (COS): a review. *Carbohydr Polym*. 2005;62(4):357–368.
9. Park JH, Lee HW, Chae DK, et al. Electrospinning and characterization of poly (vinyl alcohol)/chitosan oligosaccharide/clay nanocomposite nanofibers in aqueous solutions. *Colloid Polym Sci*. 2009;287(8):943–950.
10. Rai M, Yadav A, Gade A. Silver nanoparticles as a new generation of antimicrobials. *Biotechnol Adv*. 2009;27(1):76–83.
11. Su YH, Yin ZF, Xin HL, et al. Optimized antimicrobial and antiproliferative activities of titanate nanofibers containing silver. *Int J Nanomedicine*. 2011;6:1579–1586.
12. Yu DG, Zhou J, Chatterton NP, Li Y, Huang J, Wang X. Polyacrylonitrile nanofibers coated with silver nanoparticles using a modified coaxial electrospinning process. *Int J Nanomedicine*. 2012;7:5725–5732.
13. Eid KA, Azzazy HM. Controlled synthesis and characterization of hollow flower-like silver nanostructures. *Int J Nanomedicine*. 2012;7:1543–1550.
14. Vargas EA, do Vale Baracho NC, de Brito J, de Queiroz AA. Hyperbranched polyglycerol electrospun nanofibers for wound dressing applications. *Acta Biomater*. 2010;6(3):1069–1078.
15. Zhu W, Guo C, Yu A, Gao Y, Cao F, Zhai G. Microemulsion-based hydrogel formulation of penciclovir for topical delivery. *Int J Pharm*. 2009;378(1–2):152–158.
16. Dreher F, Walde P, Luisi PL, Elsner P. Human skin irritation studies of a lecithin microemulsion gel and of lecithin liposomes. *Skin Pharmacol*. 1996;9(2):124–129.
17. Draize JH, Woodard G, Calvery HO. Methods for the study of irritation and toxicity of substances applied topically to the skin and mucous membranes. *J Pharmacol Exp Ther*. 1944;82(3):377–390.
18. Zhao Y, Zhou Y, Wu X, Wang L, Xu L, Wei S. A facile method for electrospinning of Ag nanoparticles/poly (vinyl alcohol)/carboxymethyl-chitosan nanofibers. *Appl Surf Sci*. 2012;258(22):8867–8873.
19. Huang HH, Ni XP, Loy GL, et al. Photochemical formation of silver nanoparticles in poly(N-vinylpyrrolidone). *Langmuir*. 1996;12(4):909–912.
20. Jeon HJ, Yi SC, Oh SG. Preparation and antibacterial effects of Ag-SiO2 thin films by sol-gel method. *Biomaterials*. 2003;24(27):4921–4928.
21. Nguyen TH, Kim YH, Song HY, Lee BT. Nano Ag loaded PVA nanofibrous mats for skin applications. *J Biomed Mater Res B Appl Biomater*. 2011;96(2):225–233.
22. Madhumathi K, Sudheesh Kumar PT, Abhilash S, et al. Development of novel chitin/nanosilver composite scaffolds for wound dressing applications. *J Mater Sci Mater Med*. 2010;21(2):807–813.
23. Kumar PT, Abhilash S, Manzoor K, Nair SV, Tamura H, Jayakumar R. Preparation and characterization of novel β-chitin/nanosilver composite scaffolds for wound dressing applications. *Carbohydr Polym*. 2010;80(3):761–767.
24. Natarajan S, Williamson D, Stiltz AJ, Harding K. Advances in wound care and healing technology. *Am J Clin Dermatol*. 2000;1(5):269–275.
25. Tijing LD, Ruelo MTG, Amarjargal A, Pant HR, Park C-H, Kim CS. One-step fabrication of antibacterial (silver nanoparticles/poly (ethylene oxide))-polyurethane bicomponent hybrid nanofibrous mat by dual-spinneret electrospinning. *Mater Chem Phys*. 2012;134(2–3):557–561.
26. Pal S, Tak YK, Song JM. Does the antibacterial activity of silver nanoparticles depend on the shape of the nanoparticle? A study of the Gram-negative bacterium Escherichia coli. *Appl Environ Microbiol*. 2007;73(6):1712–1720.
27. Martinez-Castanon GA, Nino-Martinez N, Martinez-Gutierrez F, Martinez-Mendoza JR, Ruiz F. Synthesis and antibacterial activity of silver nanoparticles with different sizes. *J Nanopart Res*. 2008;10(8):1343–1348.